

Vibrational Spectroscopy of Small $\text{Br}^- \cdot (\text{H}_2\text{O})_n$ and $\text{I}^- \cdot (\text{H}_2\text{O})_n$ Clusters: Infrared Characterization of the Ionic Hydrogen Bond

Patrick Ayotte, Christopher G. Bailey, Gary H. Weddle,[†] and Mark A. Johnson*

Sterling Chemistry Laboratory, Yale University, New Haven, Connecticut 06520-8107

Received: December 1, 1997; In Final Form: March 2, 1998

We report the mid-infrared (3200–3800 cm^{-1}) vibrational predissociation spectra of the $\text{Br}^- \cdot \text{W}_n$ and $\text{I}^- \cdot \text{W}_n$ ($\text{W} = \text{H}_2\text{O}$; $1 \leq n \leq 6$) clusters, as well as several mixed solvent cases, $\text{I}^- \cdot \text{W} \cdot \text{M}$ [$\text{M} = \text{Ar}$, CH_3I , $(\text{CH}_3)_2$], involving the iodide monohydrate. While the spectra of the pure monomers and dimers are quite dependent on the halogen, the envelopes become similar by the trimers, with the larger clusters displaying a very wide, unresolved band reminiscent of the bulk water spectrum. There is a general blue shift of the band maxima with increasing solvation in both systems, an effect consistent with the strengthening of the inter-water hydrogen-bonding network at the expense of the ionic hydrogen bonds.

I. Introduction

The molecular nature of halide ion hydration has recently enjoyed a resurgence of interest as theoretical and experimental techniques become available for application to moderately sized ($n \leq 6$) gas-phase clusters.^{1–6} A recurrent theme in this endeavor has been the issue of whether anions are solvated within a shell of solvent molecules, as expected from the structure of the bulk,⁷ or whether the solvent forms a network which then binds to the anion, creating a “surface-solvated” ion.^{1a,2,4,8} Recent calculations,^{4c} for example, indicate that the coarse morphology (i.e., surface or internal solvation) adopted by the clusters is actually a sensitive test of the interaction potentials. We have previously approached the small cluster regime in the iodide–water system ($\text{I}^- \cdot \text{W}_n$, $0 \leq n \leq 4$)⁶ using UV spectroscopy to follow the evolution of the charge-transfer-to-solvent (CTTS) electronic bands⁹ in the vicinities of the $\text{I}^- \cdot \text{W}_n$ electron detachment thresholds.⁵ That work revealed the emergence of a bound electronically excited state already at $n = 3$, at odds with a prediction from *ab initio* calculations.² This apparent inconsistency is resolved, however, when one considers the spectroscopic consequences of the calculated ground-state structures. For example, the trimer is thought^{1a,2,4,8} to occur with a cyclic water network where all three hydrogens are bound to the iodide. Such a configuration possesses a very large vertical (electric) dipole moment (i.e., of the neutral at the equilibrium geometry of the anion) and therefore supports a diffuse, dipole-bound excited state, which would not have been recovered at the level of theory [MP2/6-31++G*]² used to deduce the ground-state structure.

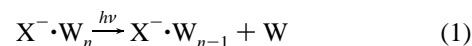
Water networks (such as the putative cyclic trimer in $\text{X}^- \cdot \text{W}_3$) should display characteristic vibrational patterns in the OH stretching region, as there is an empirical correlation¹⁰ between the red shifting of bands and the local hydrogen-bonding environment. The locations of OH stretching quanta have historically been classified into three distinct binding motifs. Water molecules with only one hydrogen engaged in H-bonding display widely spaced bands, one near 3700 cm^{-1} (correspond-

ing to the weak free OH stretch), and another, much more intense “single-donor” OH stretch, red shifted down to the 3300–3400 cm^{-1} range. Water molecules with both hydrogens participating in H-bonding (so-called “double-donors”) tend to display vibrations in the intermediate (3500–3650 cm^{-1}) region. In this paper, we survey the low-resolution (3 cm^{-1} bandwidth) mid-infrared vibrational predissociation spectra of the small $\text{I}^- \cdot \text{W}_n$ clusters and compare their behavior to that displayed by $\text{Br}^- \cdot \text{W}_n$ and the previously reported $\text{Cl}^- \cdot \text{W}_n$ system.^{1a}

II. Experimental Section

Cluster anions are synthesized in a pulsed free jet expansion and mass selected in a tandem time-of-flight spectrometer described previously.¹¹ The vapor over a (room temperature) mixture of CH_3I or CH_2Br_2 and H_2O is pressurized with 5 atm of argon and expanded through a pulsed nozzle (0.030 in. diameter, General Valve) to generate the $\text{I}^- \cdot \text{W}_n$ and $\text{Br}^- \cdot \text{W}_n$ complexes, respectively. Infrared photoexcitation is carried out at the transient focus of our tandem mass spectrometer¹¹ using a KTP-based optical parametric oscillator (Laser Vision). This laser first generates tunable near-IR radiation (1.5–2.1 μm), which is then converted to the 3–4 μm range by parametric amplification with the Nd:YAG fundamental, yielding about 5 mJ/pulse in the mid-IR with a bandwidth of about 3 cm^{-1} . Spectra are normalized to variations in the laser fluence.

Action spectra are collected by monitoring the production of fast “photoneutrals”:



which are isolated by repelling the parent and fragment anions just before they hit the detector (Galileo microchannel plate). To distinguish the H_2O photoproducts (eq 1) from the neutrals created by either collision-induced dissociation or spontaneous decay, we irradiate the clusters while they are inside a small region held at high potential (+15 kV). The resulting “photoneutrals” are therefore labeled with a unique velocity, making them readily distinguishable from non-laser-induced neutrals since the latter are largely generated outside the short high-voltage region. This strategy results in background-free detection since one can arbitrarily change the acceleration voltage

[†] Department of Chemistry, Fairfield University, Fairfield, CT 06430.

* Corresponding author. E-mail: mark.johnson@yale.edu. Fax: (203) 432-6144.

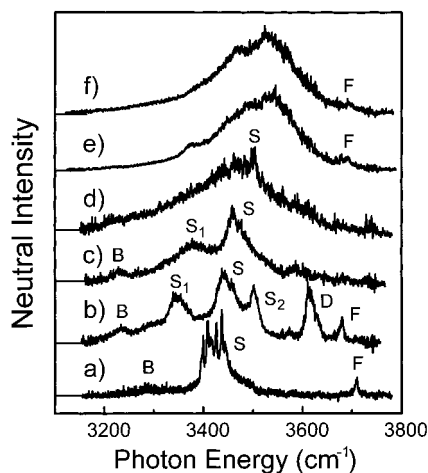


Figure 1. Vibrational predissociation spectra for (a) $\text{I}^- \cdot \text{W}_1$,^{1b,13} (b) $\text{I}^- \cdot \text{W}_2$, (c) $\text{I}^- \cdot \text{W}_3$, (d) $\text{I}^- \cdot \text{W}_4$, (e) $\text{I}^- \cdot \text{W}_5$, and (f) $\text{I}^- \cdot \text{W}_6$. Labels indicate tentative assignment to bending overtones (B), ionic H-bonded OH stretches (S), inter-water H-bonded OH stretches (D), and free OH stretches (F).

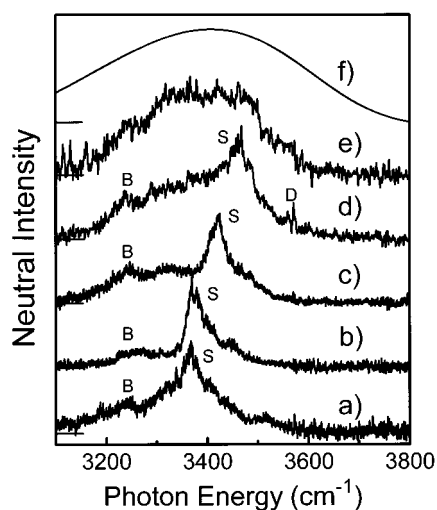


Figure 2. Vibrational predissociation spectra for (a) $\text{Br}^- \cdot \text{W}$, (b) $\text{Br}^- \cdot \text{W}_2$, (c) $\text{Br}^- \cdot \text{W}_3$, (d) $\text{Br}^- \cdot \text{W}_4$, (e) $\text{Br}^- \cdot \text{W}_5$. (f) is the absorption spectrum of liquid water at 30 °C.¹² Labels indicate tentative assignment to bending overtones (B), ionic H-bonded OH stretches (S), and inter-water H-bonded OH stretches (D).

so that the photoproducts hit the detector in a quiet region of the arrival time distribution (i.e., well before the parent ions). The time window for decomposition could be varied between 5 and 10 μs (the drift time between excitation and detection) to ensure that the fragmentation spectra were not strongly affected by kinetic shifts.

III. Results and Discussion

III.A. Survey Spectra of the $\text{Br}^- \cdot \text{W}_n$ and $\text{I}^- \cdot \text{W}_n$, $1 \leq n \leq 6$, Cluster Anions. The vibrational predissociation spectra of the $\text{I}^- \cdot \text{W}_n$ and $\text{Br}^- \cdot \text{W}_n$ clusters are presented in Figures 1 and 2, respectively. In each case, the small ($n = 1, 2, 3$) clusters display relatively sharp features that give way to a very broad, unresolved band by $n = 5$. This broad structure is reminiscent of the bulk water spectrum in this region, which is included in the top trace (f) in Figure 2.¹² The spectral density generally blue shifts with increasing hydration in both systems. The similarity of the $\text{X}^- \cdot \text{W}_3$ profiles is striking in light of the distinct halide dependence of the $n = 1$ and 2 spectra (a and b in Figures 1 and 2, respectively). We have labeled bands (or local maxima)

TABLE 1: Frequencies ($\pm 3 \text{ cm}^{-1}$) of the Vibrational Features Labeled in Figures 1 and 2

n	band label	frequency	
		$\text{Br}^- \cdot \text{W}_n$	$\text{I}^- \cdot \text{W}_n$
1	B	3241	3295
	S	3368	3420
	F		3710
2	B	3250	3232
	S	3373	3440
	S_1		3347
	S_2		3502
	D		3615
3	F		3680
	B	3244	3231
	S	3422	3459
4	S_1		3380
	B	3245	
	S	3466	3501
5, 6	D	3567	
	F		3690

that appear to be empirically related to one another and collected them in Table 1. The labels correspond to assignments of the bands to bend overtones (B), ionic H-bonded OH stretches (S), inter-water H-bonded OH stretches (D), and free OH stretches (F).

III.B. Comparison of the Monohydrates $\text{X}^- \cdot \text{W}$, for $\text{X} = \text{Cl}, \text{Br},$ and I . Both $\text{I}^- \cdot \text{W}^{1b,13}$ and $\text{Br}^- \cdot \text{W}$ spectra (Figures 1a and 2a, respectively) display strong bands in the single-donor region, with the iodine showing much sharper features and richer fine structure. Some of this difference in profile surely results from the higher $\text{Br}^- \cdot \text{W}$ bond dissociation energy relative to $\text{I}^- \cdot \text{W}$ ($4100 \pm 150 \text{ cm}^{-1}$ vs $3600 \pm 110 \text{ cm}^{-1}$)^{14–16} so that the one-photon $\text{Br}^- \cdot \text{W}$ action spectrum results from excitation of warmer clusters than that for $\text{I}^- \cdot \text{W}$. The free OH stretch is clear in the $\text{I}^- \cdot \text{W}$ spectrum, but is obscured, if present, in the $\text{Br}^- \cdot \text{W}$ spectrum, possibly due to the lower signal-to-noise ratio in the latter case.

The localization of the $\text{X}^- \cdot \text{W}$ ($\text{X} = \text{Br}, \text{I}$) spectral density in the $3300\text{--}3400 \text{ cm}^{-1}$ range is consistent with the calculated minimum energy structures for these complexes, where the water molecule adopts a C_s geometry (i.e., cocked with one H pointing toward the halide).^{1a,4} Consequently, the vibrational spectrum displays a strong ionic H-bonded OH stretch at low energy ($3300\text{--}3400 \text{ cm}^{-1}$) and a much weaker free OH stretch ($\sim 3700 \text{ cm}^{-1}$) near the average of the free water bands (3652 and 3756 cm^{-1} for ν_1 and ν_3 , respectively). It is well-known that the ionic H-bonded OH stretch has a large dipole derivative and, therefore, usually dominates the IR spectrum.^{1a,4} (For comparison, a C_{2v} isomer would display two bands of comparable intensity in the middle of the OH stretch region [$3500\text{--}3650 \text{ cm}^{-1}$].)

The most obvious qualitative difference between the $\text{Br}^- \cdot \text{W}$ and $\text{I}^- \cdot \text{W}$ spectra is that the single-donor OH stretch in the former is red shifted by about 50 cm^{-1} relative to the iodide. We have previously established¹³ that the band location in $\text{I}^- \cdot \text{W}$ is not an artifact of the (undefined) cluster temperature by observing the band via predissociation of a very weakly bound “spy” such as Ar (Figure 4b). While one might suspect that the band shift in $\text{Br}^- \cdot \text{W}$ results from a temperature effect, we note that this red shifting trend continues in $\text{Cl}^- \cdot \text{W}$, whose one-photon spectrum has recently been acquired by Okumura’s group, using CCl_4 as a spy molecule.¹⁷ In fact, the $\text{Br}^- \cdot \text{W}$ data now enable us to establish an empirical trend in the single donor frequency relative to the strength of the ionic H-bond down the halogen series. This is displayed in Figure 3, where we plot the experimentally determined OH stretching frequencies

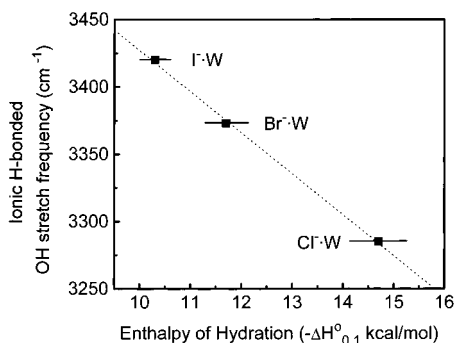


Figure 3. Comparison of the ionic H-bonded OH stretch frequencies as a function of the experimental enthalpy of solvation^{14–16} for the chloride (Cl⁻·W),^{1a,17} bromide (Br⁻·W), and iodide (I⁻·W)^{1b,13} mono-hydrates.

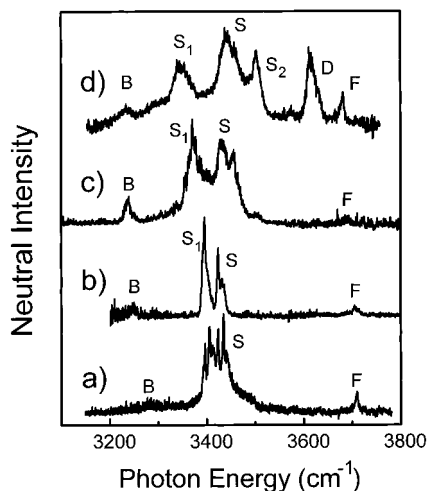


Figure 4. Vibrational predissociation spectra for (a) I⁻·W,^{1b,13} (b) I⁻·W·Ar,¹³ (c) I⁻·W·CH₃I, and (d) I⁻·W₂. Labels indicate tentative assignment to bending overtones (B), ionic H-bonded OH stretches (S), inter-water H-bonded OH stretches (D), and free OH stretches (F).

against the X⁻ enthalpies of hydration (ΔH_{0,1}) determined from high-pressure mass spectrometry.^{14–16} The fact that Br⁻·W falls exactly as expected from interpolation between the other two halides strongly suggests that this value is not a consequence of temperature, but rather reflects an intrinsic feature of the ionic H-bond. We also note that, like Br⁻·W, the free OH stretch band was also absent in the Cl⁻·W spectrum. The feature was recovered, however, using CCl₄ predissociation,^{17,18} verifying that this complex is indeed asymmetric (C_s symmetry with one hydrogen free). The small intensity of the free OH is in line with calculations,^{1a,4,17} indicating that it is 10–30 times weaker than the ionic H-bond.

The evolution of the ionic hydrogen bond down the halides has been explored using ab initio calculations which, in turn, yield a more detailed view of how this correlation reflects the character of the bond. Xantheas's calculations at the MP2/MP4 (aug-cc-pVDZ/aug-cc-pVTZ basis set) level,⁴ for example, show a pronounced decrease in equilibrium X⁻–H–O angle down the halogen series (177°, 168°, and 165° for X = F, Cl, and Br, respectively)^{4,19} along with a decrease in H-bonded OH bond length (R_{OH} = 1.055, 0.992, and 0.987 Å for X = F, Cl, and Br, respectively, compared to a bond length of 0.966 Å for the free water molecule calculated at the same level of theory). This loss in directionality with increasing X⁻ radius indicates a weakening of the H-bond, and as the water molecule relaxes back toward its unperturbed (i.e., free water) geometry, the ionic H-bonded OH stretching vibration blue shifts back toward the

unperturbed value.²⁰ Xantheas has also found another empirical relationship between the shift in the OH stretch and the elongation of the intramolecular bond in a manner anticipated by Badger's rule.²¹

III.C. Effect of a Second Solvent Molecule: Predissociation of I⁻·W·M; M = Ar, CH₃I, (CH₃I)₂. As we mentioned above, complexation of I⁻·W with Ar has very little effect on the vibrational pattern, as expected, since the argon matrix shifts for ions tend to be rather small (10–40 cm⁻¹).²² The primary changes occur in the partially resolved fine structure of the vibrational bands and a small red shift (~5 cm⁻¹)¹³ of the band center (i.e., median at half-maximum). The spectra are reproduced in Figure 4a,b for direct comparison. Shortly we will be discussing the spectra of water dimers on Br⁻ and I⁻, where the solvent molecules have the opportunity to H-bond to each other as well as to the ion. We first consider the related case where we have a second solvent molecule strongly bound to the ion, but which will not participate in H-bonding to the water.

Methyl iodide (CH₃I) is a good candidate to explore the strong binding regime since its dipole moment (1.62 D) is comparable to that of water (1.8 D) and they have similar binding energies to iodide [10.3 ± 0.3^{14–16} vs 9.0 ± 0.2²³ kcal/mol for H₂O and CH₃I, respectively]. The action spectrum for predissociation of the I⁻·W·CH₃I complex is shown in Figure 4c. Since the CH₃I fundamentals lie outside of this spectral range, we conclude that the transitions arise from excitation of water. Again, the spectrum is dominated by an intense single-donor band, somewhat broader than that obtained for the Ar complex (fwhm's ~120 vs ~60 cm⁻¹). The band center is red shifted by only ~15 cm⁻¹ compared to the I⁻·W complex, indicating that the local H-bond between water and the ion is not strongly perturbed by the almost equally strong bond to CH₃I. Interestingly, the quartet in the I⁻·W spectrum is quenched to a doublet with the addition of an argon atom, while CH₃I further splits this doublet. Unfortunately, despite the fact that we have obtained the spectrum of the I⁻·HDO species,¹³ the assignment of this doublet remains unclear.

The free OH stretch (band F in Figure 4c) in I⁻·W·CH₃I is red shifted by a similar amount (~20 cm⁻¹) as the single donor relative to I⁻·W. A rather intense new band also appears very far to the red at 3232 cm⁻¹. A band in this vicinity (3156 cm⁻¹) was found in the Cl⁻·W complex and assigned to the overtone of the water bend.^{1a,17} In another study, Mikami and co-workers²⁴ identified a band at 3236 cm⁻¹ in the phenol·W_n system and similarly assigned it to the bend overtone. The fact that the latter gains intensity in I⁻·W·CH₃I suggests that the water is somewhat perturbed by the other solvent molecule. We have also added a second CH₃I to form the I⁻·W·(CH₃I)₂ quaternary complex (not shown). The ionic H-bonded OH stretch and the putative bend are largely unaffected by the second CH₃I. The peak locations for the various complexes are gathered in Table 2.

III.D. Decay Dynamics of I⁻·W·CH₃I upon Excitation of the Water: Statistical Decomposition. The similarity in binding energy between CH₃I and water also allows us to test whether energy initially localized in the water molecule is randomized throughout the complex prior to dissociation by monitoring the fragment distribution. The photofragments from excitation of the H-bonded OH stretch (hν = 3373 cm⁻¹) are shown in Figure 5. The ionic fragments are dominated by loss of the CH₃I molecule (branching ratio ~ 0.93) with a small contribution from loss of water (branching ratio ~ 0.07), as expected for thermal dissociation rather than prompt rupture of the I⁻·W bond upon excitation of the ionic H-bond.

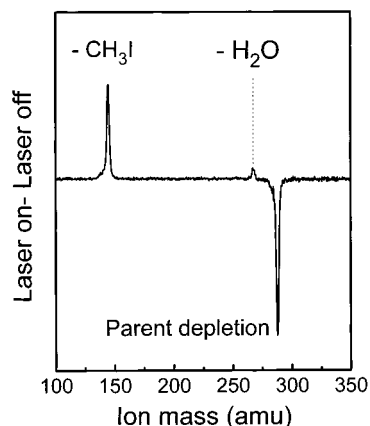


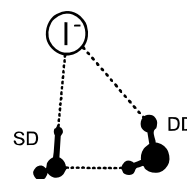
Figure 5. Laser on-laser off photofragmentation spectrum of the $\text{I}^- \cdot \text{W} \cdot \text{CH}_3\text{I}$ clusters upon excitation of the ionic H-bonded OH stretch at 3373 cm^{-1} . The fragmentation pattern indicates that evaporation of CH_3I is the dominant decay pathway, as would be expected for statistical decomposition of $\text{I}^- \cdot \text{W} \cdot \text{CH}_3\text{I}$.

TABLE 2: Frequencies ($\pm 3 \text{ cm}^{-1}$) of the Vibrational Features Labeled in Figure 4

	band label	frequency
$\text{I}^- \cdot \text{W}^{1b,13}$	B	3295
	S	3420
	F	3710
$\text{I}^- \cdot \text{W} \cdot \text{Ar}^{13}$	B	3247
	S	3423
	S_1	3395
	F	3705
	S_2	3433
$\text{I}^- \cdot \text{W} \cdot \text{CH}_3\text{I}$	B	3238
	S	3433
	S_1	3372
	F	3690
	S_2	3440
$\text{I}^- \cdot \text{W}_2$	B	3232
	S	3440
	S_1	3347
	S_2	3502
	D	3615
	F	3680

III.E. $\text{X}^- \cdot \text{W}_2$ Clusters; $\text{X} = \text{Br}$ and I . The critical issue in the doubly solvated clusters is the relation between the two solvent molecules. Their disposition reflects a delicate balance between the directional H-bond of each water to the ion, favoring a symmetrical arrangement, and H-bonding between the waters, leading to an asymmetrically solvated halide. For example, the $\text{H}_1-\text{X}-\text{H}_2$ angle is calculated⁴ to decrease dramatically down the halides (96° , 67° , and 63° , for F^- , Cl^- , and Br^- , respectively), making it more likely to observe inter-solvent H-bonding for the heavier halides. This emergence of inter-water binding provides a compelling context in which to discuss the differences between the experimentally determined $\text{Br}^- \cdot \text{W}_2$ and $\text{I}^- \cdot \text{W}_2$ spectra in Figures 1b and 2b, respectively. The $\text{Br}^- \cdot \text{W}_2$ spectrum is quite similar to that of the $\text{Br}^- \cdot \text{W}$ monomer (Figure 2a), suggesting that the two water molecules are more or less equivalent, as would be the case for symmetrical solvation. The $\text{I}^- \cdot \text{W}_2$ spectrum, however, is completely different than that of its monomer (Figure 1a) with many bands spread throughout the region. Further, we know that this difference cannot be attributed to solvent perturbation alone (mediated by the polarizability of I^- , for example) since there are features in this spectrum not present in the $\text{I}^- \cdot \text{W} \cdot \text{CH}_3\text{I}$ mixed solvent case (Figure 4c). As we expect that the ionic H-bond to water is weakest in the iodide complex, it is logical to seek an explanation of the bands unique to $\text{I}^- \cdot \text{W}_2$ based on the emergence of the inter-solvent H-bond. As we mentioned in

the Introduction, we have already appealed to this asymmetric structure² involving two dissimilar water molecules, denoted SD (single donor) and DD (double donor),



in our earlier work⁶ on the emergence of the CTTS band in the UV.

We find it useful to consider the band assignments of the $\text{I}^- \cdot \text{W}_2$ complex in the context of Figure 4, which displays this spectrum along with those of the $\text{I}^- \cdot \text{W} \cdot \text{Ar}$ and $\text{I}^- \cdot \text{W} \cdot \text{CH}_3\text{I}$ complexes. The most obvious difference between these spectra is that the $\text{I}^- \cdot \text{W}_2$ complex displays an intense band (D) completely absent in the other spectra. It occurs in the expected region for an inter-water H-bond arising from the DD water and unambiguously indicates that the two water molecules are linked together. Bands B, S, and S_1 are already present in the case of the $\text{I}^- \cdot \text{W} \cdot \text{CH}_3\text{I}$ clusters, suggesting their assignment to the SD water, with bands B and F arising from the bending overtone and the free OH, respectively. Band S_1 in $\text{I}^- \cdot \text{W}_2$ falls in line with the empirical position of band S_1 (the lower energy member of the single-donor doublet) in the argon and methyl iodide complexes, as it red shifts with increasing binding energy of the second solvent molecule. Band S is basically unperturbed in all three complexes, so that the doublet pattern opens as bands S and S_1 split apart. A new band (S_2) appears in this region for $\text{I}^- \cdot \text{W}_2$ and likely results from the ionic H-bonded OH in the DD water, which rotates away from its monomer H-bond angle to accommodate the inter-water H-bond. Clearly, both water molecules might display the doublet signature (i.e., S and S_1 in $\text{I}^- \cdot \text{W} \cdot \text{CH}_3\text{I}$), and one suspects that the breadth of band S arises from a blended structure. Thus, with the $\text{I}^- \cdot \text{W} \cdot \text{CH}_3\text{I}$ complex as a guide, all the observed bands in $\text{I}^- \cdot \text{W}_2$ can be empirically traced to vibrations of one single-donor and one double-donor water molecule. Clearly, double resonance and isotopic labeling, coupled with ab initio theory, will likely be required to pin down these assignments.

III.F. $\text{X}^- \cdot \text{W}_n$ Clusters; $n > 2$, $\text{X} = \text{Br}$ and I . In light of the differences in the dimer spectra, it is curious that the $\text{X}^- \cdot \text{W}_3$ spectra are so similar (Figures 1c and 2c). Both show a dominant feature with a broad shoulder toward lower energy and a faster falloff toward higher energy. The relatively strong free OH band in $\text{I}^- \cdot \text{W}_2$ is absent in the trimer, suggesting that all hydrogens are engaged in H-bonding. All calculations agree^{1a,2,4,8} that the global maxima of the $\text{X}^- \cdot \text{W}_3$ ($\text{X} = \text{Cl}$, Br , I) clusters involve a cyclic water trimer with all "free" hydrogens pointed toward the halide. A planar transition state (all oxygen atoms and the halide anion lying in the same plane) lies higher in energy with increasing halide size (the barrier is calculated to be very small for fluorine).⁴ The similarity of the $\text{Br}^- \cdot \text{W}_3$ and $\text{I}^- \cdot \text{W}_3$ spectra indicate that both species possess this motif which, in turn, indicates that inter-water bonding has overcome the individual $\text{X}^- \cdot \text{W}$ ionic H-bonds.

The profiles become even more similar by the tetramers, which are degraded to the red with a blue-shifted band maximum relative to the trimers. Again, calculations agree that the crown arrangement, where four water molecules form a cyclic network, "surface-bound" halide isomer, is the global minimum.^{1a,2,4,8} In such cases, all solvent molecules act as double donors and the spectral density of these isomers should appear in the intermedi-

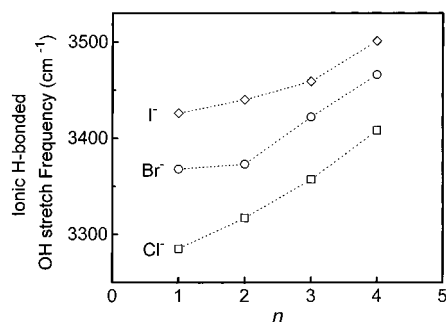


Figure 6. Comparison of the frequencies of the band maxima (band S) as a function of the number of water ligands, n , for (□) chloride ($\text{Cl}^- \cdot \text{W}_n$),^{1a,17} (○) bromide ($\text{Br}^- \cdot \text{W}_n$), and (◇) iodide ($\text{I}^- \cdot \text{W}_n$) clusters.

ate range (3500–3650 cm^{-1}). We caution, however, that the larger clusters almost certainly contain significant internal energy, approaching the evaporative cooling limit, and the broad spectral profile may result from a fluctuating ensemble. Such effects have been simulated, for example, by Garrett,²⁵ who carried out molecular dynamics calculations on the $\text{Cl}^- \cdot \text{W}_n$ and $\text{I}^- \cdot \text{W}_n$ systems to explore the issue of surface vs internal solvation in clusters with finite temperature.

III.G. Evolution of the Ionic Hydrogen Bond Strength with Solvation: Trends down the Halide Series. The blue shift of the ionic H-bonded OH stretch with increasing number of water ligands reported here for the $\text{Br}^- \cdot \text{W}_n$ and $\text{I}^- \cdot \text{W}_n$ clusters was also observed by Okumura and co-workers^{1a} in the $\text{Cl}^- \cdot \text{W}_n$ system. They attributed this effect to the weakening of the ionic H-bond as more solvent molecules bind to the ion (without necessarily binding with each other).¹⁷ To explore this effect, we plot the energies of the band maxima (band S) as a function of the number of water ligands in Figure 6 for the solvated chloride (squares), bromide (circles), and iodide (diamonds) anions. Interestingly, the stronger H-bond in the $\text{Cl}^- \cdot \text{W}_n$ system is also the most blue shifted (and presumably weakened) with the formation of the water–water network (suggested to occur at $n = 4$).^{1a,17} The $\text{I}^- \cdot \text{W}_n$ system, on the other hand, which already has a weaker bond to a single water molecule, suffers less reduction upon formation of the water subclusters, leading to a smaller proportional shift.

IV. Conclusion

Vibrational spectroscopy of the $\text{Br}^- \cdot \text{W}_n$ and $\text{I}^- \cdot \text{W}_n$ clusters reveals multiple band origins for $n \leq 3$ which merge into a broad band for the larger clusters. The spectral density generally blue shifts with increasing solvation, an effect consistent with weakening of the ionic H-bonds upon formation of water networks. The differences between $\text{Br}^- \cdot \text{W}_2$ and $\text{I}^- \cdot \text{W}_2$ are striking. The bromide appears to be formed by two equivalent waters, while the spectrum of $\text{I}^- \cdot \text{W}_2$ is unique, indicating the presence of two dissimilar water molecules. This onset of interwater bonding at the dimer for iodide is correlated with the fact that the ionic H-bond is weakest for this largest halide of the series. Finally, we report an empirical trend in the frequency of the H-bonded OH stretching quanta with the binding energies of the monomeric complexes.

Acknowledgment. We thank Dr. S. Xantheas and Profs. B. Gerber, M. Okumura, and J. Lisý for valuable discussions on

the assignments of bands, as well as access to unpublished work. We also thank the National Science Foundation for support of this work, as well as the NEDO foundation. P.A. acknowledges support from FCAR.

References and Notes

- (1) (a) Okumura, M.; Choi, J.-H.; Kuwata, K. T.; Cao, Y.-B.; Haas, B.-M. *SPIE Proceedings*; San Diego CA, 1995; p 147. (b) Johnson, M. S.; Kuwata, K. T.; Wong, C.-K.; Okumura, M. *Chem. Phys. Lett.* **1996**, *260*, 551.
- (2) Combariza, J. E.; Kestner, N. R.; Jortner, J. *Chem. Phys. Lett.* **1993**, *203*, 423. Combariza, J. E.; Kestner, N. R.; Jortner, J. *J. Chem. Phys.* **1994**, *100*, 2851.
- (3) Zhao, X. G.; Gonzales-Lafont, A.; Truhlar, D. G.; Steckler, R. *J. Chem. Phys.* **1991**, *94*, 5544. Hu, W. P.; Truhlar, D. G. *J. Phys. Chem.* **1994**, *98*, 1049.
- (4) (a) Xantheas, S. S. *J. Phys. Chem.* **1996**, *100*, 9703. (b) Xantheas, S. S.; Dunning, T. H. *J. Phys. Chem.* **1994**, *98*, 13489. (c) Xantheas, S. S.; Dang, L. X. *J. Phys. Chem.* **1996**, *100*, 3989.
- (5) Markovich, G.; Pollack, S.; Giniger, R.; Cheshnovsky, O. *J. Chem. Phys.* **1994**, *102*, 9344. Markovich, G.; Giniger, R.; Levin, M.; Cheshnovsky, O. *Z. Phys. D* **1991**, *20*, 69. Markovich, G.; Giniger, R.; Levin, M.; Cheshnovsky, O. *J. Chem. Phys.* **1991**, *95*, 9416.
- (6) Serxner, D.; Dessent, C. E. H.; Johnson, M. A. *J. Chem. Phys.* **1996**, *105*, 7231.
- (7) Marcus, Y. *Ion Solvation*; Wiley: New York, 1985.
- (8) Perera, L.; Berkowitz, M. L. *J. Chem. Phys.* **1991**, *95*, 1954. Perera, L.; Berkowitz, M. L. *J. Chem. Phys.* **1992**, *96*, 8288. Perera, L.; Berkowitz, M. L. *Z. Phys. D* **1993**, *26*, 166. Perera, L.; Berkowitz, M. L. *J. Chem. Phys.* **1993**, *99*, 4222. Perera, L.; Berkowitz, M. L. *J. Chem. Phys.* **1993**, *99*, 4236. Perera, L.; Berkowitz, M. L. *J. Chem. Phys.* **1994**, *100*, 3085. Sremaniak, L. S.; Perera, L.; Berkowitz, M. L. *Chem. Phys. Lett.* **1994**, *218*, 377. Yeh, I.-C.; Perera, L.; Berkowitz, M. L. *Chem. Phys. Lett.* **1997**, *264*, 31.
- (9) Fox, M. F.; Hayon, E. *J. Chem. Soc., Faraday Trans. 1* **1977**, *73*, 1003.
- (10) Kim, K.; Jordan, K. D.; Zwier, T. S. *J. Am. Chem. Soc.* **1994**, *116*, 11568. Pribble, R. N.; Zwier, T. S. *Science* **1994**, *265*, 75.
- (11) Johnson, M. A.; Lineberger, W. C. In *Techniques for the Study of Gas-Phase Ion-Molecule Reactions*; Farrar, J. M., Saunders, W., Eds.; Wiley: New York, 1988; p 591.
- (12) Walrafen, G. E. *J. Chem. Phys.* **1967**, *47*, 114.
- (13) Bailey, C. G.; Kim, J.; Dessent, C. E. H.; Johnson, M. A. *Chem. Phys. Lett.* **1997**, *269*, 122.
- (14) Kebarle, P.; Arshadi, M.; Scarborough, J. J. *J. Chem. Phys.* **1968**, *49*, 817. Arshadi, M.; Yamdagni, R.; Kebarle, P. *J. Phys. Chem.* **1970**, *74*, 1475.
- (15) Hiraoka, K.; Mizuse, S.; Yamabe, S. *J. Phys. Chem.* **1988**, *92*, 3943.
- (16) Keese, R. G.; Castleman, A. W., Jr. *J. Chem. Phys. Lett.* **1980**, *74*, 139. Keese, R. G.; Castleman, A. W., Jr. *J. Phys. Chem. Ref. Data* **1986**, *15*, 1011.
- (17) Choi, J.-H.; Kuwata, K. T.; Cao, Y.-B.; Okumura, M. *J. Phys. Chem. A* **1998**, *102*, 503.
- (18) The absence of a free OH band has been attributed to the large anharmonicity of this mode in the hypothetical case where the clusters would decay via two-photon dissociation (For $\text{Cl}^- \cdot \text{W}$, $\Delta H_{0,1} = 5100 \pm 200 \text{ cm}^{-1}$).^{14–16}
- (19) Zhan, C.-G.; Iwata, S. *Chem. Phys. Lett.* **1995**, *232*, 72.
- (20) The calculated shifts⁴ are ~ 1500 , ~ 510 , and $\sim 400 \text{ cm}^{-1}$ with respect to the free OH stretch for $\text{F}^- \cdot \text{W}$, $\text{Cl}^- \cdot \text{W}$, and $\text{Br}^- \cdot \text{W}$, respectively, overestimating the experimental shifts by 25%.
- (21) Herzberg, G. H. *Molecular Spectra and Molecular Structure I. Spectra of Diatomic Molecules*; Van Nostrand Reinhold: New York, 1950; p 457.
- (22) Jacox, M. E. *Chem. Phys.* **1994**, *189*, 149. Forney, D.; Jacox, M. E.; Thompson, W. E. *J. Mol. Spectrosc.* **1993**, *157*, 479.
- (23) Dougherty, R. C.; Dalton, J.; Roberts, J. D. *Org. Mass Spectrosc.* **1974**, *8*, 77.
- (24) Tanabe, S.; Ebata, T.; Fujii, M.; Mikami, N. *Chem. Phys. Lett.* **1993**, *215*, 347.
- (25) Dang, L. X.; Garrett, B. C. *J. Chem. Phys.* **1993**, *99*, 2972. Gai, H.; Dang, L. X.; Schenter, G. K.; Garrett, B. C. *J. Phys. Chem.* **1995**, *99*, 13303.